AMERICAN SOCIETY FOR MICROBIOLOGY | Applied and Environmental Microbiology®

MICROBIAL ECOLOGY

A Large Tn*7*-like Transposon Confers Hyperresistance to Copper in *Pseudomonas syringae* pv. syringae

Francesca Aprile,[a] Zaira Heredia-Ponce,[a] Francisco M. Cazorla,[a] Antonio de Vicente,[a] José A. Gutiérrez-Barranquero[a]

[a]Instituto de Hortofruticultura Subtropical y Mediterránea La Mayora (IHSM-UMA-CSIC), Departamento de Microbiología, Facultad de Ciencias, Universidad de Málaga, Málaga, Spain

ABSTRACT Copper resistance mechanisms provide an important adaptive advantage to plant-pathogenic bacteria under exposure to copper treatments. Copper resistance determinants have been described in *Pseudomonas syringae* pv. syringae (Pss) strains isolated from mango intimately associated with 62-kb plasmids belonging to the pPT23A family (PFP). It has been previously described that the indiscriminate use of copper-based compounds promotes the selection of copper-resistant bacterial strains and constitutes a selective pressure in the evolution of copper resistance determinants. Hence, we have explored in this study the copper resistance evolution and the distribution of specific genetic determinants in two different Pss mango populations isolated from the same geographical regions, mainly from southern Spain, with an average of 20 years of difference. The total content of plasmids, in particular the 62-kb plasmids, and the number of copper-resistant Pss strains were maintained at similar levels over time. Interestingly, the phylogenetic analysis indicated the presence of a phylogenetic subgroup (PSG) in the Pss mango phylotype mostly composed of the recent Pss population analyzed in this study that was strongly associated with a hyperresistant phenotype to copper. Genome sequencing of two selected Pss strains from this PSG revealed the presence of a large Tn*7*-like transposon of chromosomal location, which harbored putative copper and arsenic resistance genes (COARS Tn*7*-like). Transformation of the copper-sensitive Pss UMAF0158 strain with some putative copper resistance genes and reverse transcription-quantitative PCR experiments brought to light the role of COARS Tn*7*-like transposon in the hyperresistant phenotype to copper in Pss.

IMPORTANCE Copper compounds have traditionally been used as standard bactericides in agriculture in the past few decades. However, the extensive use of copper has fostered the evolution of bacterial copper resistance mechanisms. *Pseudomonas syringae* is a plant-pathogenic bacterium used worldwide as a model to study plant-pathogen interactions. The adaption of *P. syringae* to plant surface environment is the most important step prior to an infection. In this scenario, copper resistance mechanisms could play a key role in improving its epiphytic survival. In this work, a novel Tn*7*-like transposon of chromosomal location was detected in *P. syringae* pv. syringae strains isolated from mango. This transposon conferred the highest resistance to copper sulfate described to date for this bacterial phytopathogen. Understanding in depth the copper resistance mechanisms and their evolution is an important step for the agricultural industry to improve disease management strategies.

KEYWORDS *Pseudomonas syringae* pv. syringae, mango host, pPT23A plasmids, copper resistance, COARS Tn*7*-like transposon

Pseudomonas syringae is a major bacterial phytopathogen used worldwide as a model bacterium to study plant-pathogen interactions (1). *P. syringae* synthesizes a vast array of virulence factors, prominent among which are the type III secretion

Citation Aprile F, Heredia-Ponce Z, Cazorla FM, de Vicente A, Gutiérrez-Barranquero JA. 2021. A large Tn*7*-like transposon confers hyperresistance to copper in *Pseudomonas syringae* pv. syringae. Appl Environ Microbiol 87:e02528-20. https://doi.org/10.1128/AEM.02528-20.

Editor Maia Kivisaar, University of Tartu

Address correspondence to José A. Gutiérrez-Barranquero, jagutierrez@uma.es.

Received 14 October 2020
Accepted 12 December 2020
Accepted manuscript posted online 23 December 2020
Published 12 February 2021

system (T3SS) and diverse toxic compounds, such as lipodepsipeptide and antimetabolite toxins (2–4). The *P. syringae* species belongs to the *P. syringae* complex, which has been described as a taxonomic hodgepodge that includes at least nine different taxonomically related species (5–7). More than 60 pathovars of *P. syringae* have been reported (7), with the pathovar syringae being the most outstanding pathovar due to its broad arsenal of virulence factors and host range (4). In addition, adaptation mechanisms have emerged as being important for colonization and survival strategies on the plant surface environment and also are closely connected with bacterial virulence (4). *P. syringae* pv. syringae (Pss) strains isolated from mango trees have been described as the causal agent of bacterial apical necrosis (BAN) disease of mango trees (8). Pss strains isolated from mango form a single phylotype within phylogenetic group 2 of the *P. syringae* complex (9), mainly associated with the mango host and with the production of the antimetabolite toxin mangotoxin (6, 10).

Copper-based compounds traditionally have been used in agriculture as standard bactericides targeting plant-pathogenic bacteria (11). However, copper is a major heavy metal, and the indiscriminate use of copper-based compounds has entailed severe environmental impact affecting soil, plants, and food security (12–14). It should be pointed out that the excessive use of copper has promoted the selection of copper-resistant strains and facilitated the evolution and spread of copper resistance determinants in many different bacteria, including *P. syringae* (15–20). In this context, mobile genetic elements, such as plasmids, integrative conjugative elements, and transposons, play an important role in bacterial evolution due to their ability to acquire foreign DNA that can be transmitted to other bacteria via horizontal gene transfer (HGT) mechanisms (21–23). In particular, plasmid DNA is considered part of the flexible genome, and plasmids tend to encode important genes that can improve the epiphytic survival and virulence of their bacterial hosts (24–26). The pPT23A-family of plasmids (PFPs) is a family of plasmids that appear to be indigenous to *P. syringae* (24), with all of them sharing a conserved major replication gene, *repA* (27). The most common genetic determinant associated with copper resistance in *P. syringae* is the *copABCD* operon, described for the first time in *P. syringae* pv. tomato (28). The *copABCD* operon and UV radiation resistance genes (*rulAB* operon) are frequently carried by PFP plasmids (24). The presence of PFP plasmids has also been reported in Pss strains isolated from mango (15, 26). Hitherto, *rulAB* genes and two different variants of copper resistance determinants have been found in Pss strains isolated from mango, carried mainly by 62-kb PFP plasmids (15, 26, 29, 30). The two copper resistance determinants are the *copABCD* operon and the *copABCD-cusCBA-copG* gene cluster (designated a *copABCD* novel structure, *copABCD*ns), which was described for the first time in a Pss strain isolated from mango (30). The detoxification mechanism of the *copABCD* operon involves copper binding by sequestering proteins, and the *cus* genes belong to the heavy-metal efflux (HME)-RND (resistance-nodulation-cell division) family. The presence of the *copABCD*ns has been demonstrated to increase copper resistance compared with that of the *copABCD* operon (30). Other than these two different variants of copper resistance determinants harbored by PFP plasmids in Pss strains isolated from mango, previous data have suggested the existence of at least another copper resistance determinant variant that can even improve the resistance to copper compounds (6, 15). Based on this premise, the main aim of this work was to elucidate the copper resistance distribution and the specific genetic determinants harbored by two different Pss populations isolated from mango from different worldwide regions, but mainly from southern Spain, and separated in time by an average of 20 years.

RESULTS

Bacterial isolates identification as *Pseudomonas syringae* pv. syringae. Eighty-two bacterial isolates from mango, comprising Pss strains isolated mainly before the year 2000 (designated population 1, or P1) and Pss strains from 2016 to 2017 (designated population 2, or P2), were collected. The P1 population comprised 38 Pss strains

isolated from mango. Seven Pss strains isolated from other hosts were included as external controls of the P1 population. The P2 population (n = 44) comprised strains recovered from mango trees with BAN symptoms isolated from the same geographical regions as the P1 population. Three Pss strains isolated from other hosts were included as external controls of the P2 population (Table 1). These 47 P2 isolates were identified as Pss through biochemical, physiological, and genetic approaches. All were fluorescent on KB medium under UV light, levan positive, cytochrome *c* oxidase negative, arginine dihydrolase negative, and positive for tobacco hypersensitive response. All isolates hydrolyzed gelatin and esculin and metabolized glucose, mannitol, inositol, adonitol, gluconate, propionate, L-lactate, and L-histidine but not L-tartrate. All isolates showed ice nucleation activity at −5°C. Gene *syrB* was detected by PCR in all isolates that also produced syringomycin. In all isolates, the presence of the *mboAB* genes, which also produced the antimetabolite toxin mangotoxin, was detected by PCR (see Fig. S1 in the supplemental material). All these tests were also repeated for the 45 P1 Pss strains to confirm their previous identifications. All the Pss strains showed the same results, with a few exceptions regarding the production of mangotoxin and the detection by PCR of *mboAB* genes. Pss ICMP14923, Pss UMAF2801, and Pss UMAF0167 strains (isolated from mango) and the Pss UMAF1444-5 strain (isolated from laurel) did not produce mangotoxin, but the presence of *mboAB* genes was detected by PCR. Pss EPSMV3, Pss UMAF6016, and Pss UMAF6582 strains were negative for PCR detection of the *mboAB* genes and for the production of mangotoxin.

Plasmid profile analysis in Pss strains isolated from mango. The plasmid content and the assessment of PFP status were studied in the P1 and P2 Pss mango populations. From the P1 population, 25 Pss strains harbored plasmids, while in the P2 population, 36 Pss strains harbored plasmids (Fig. 1A). Five different plasmid profiles were found in both Pss populations (45 kb, 62 kb, 120 kb, 45 to 62 kb, and 62 to 88 kb). The plasmid profile 45 to 120 kb was detected only in the P2 strain UMAF0292. The 62-kb plasmid profile was the most represented, being present in 17 and 24 Pss strains from P1 and P2, respectively (Fig. 1B). The 120-kb plasmid profile was the second most represented plasmid profile and was present in 2 Pss strains from P1 and in 5 Pss strains from P2 (Fig. 1B). The number of plasmids present in the P2 population with respect to the P1 population, in particular the 62-kb plasmids, was not statistically different according to a Pearson chi-squared test. Therefore, the total content of plasmids was maintained at similar levels between P1 and P2 populations. Southern blot hybridizations with *repA* and *rulA* genes were performed to determine which plasmids belonged to the PFP family (Table S1). Southern blot experiments with the *repA* gene probe demonstrated that the 62-kb plasmid always belonged to the PFP family when harbored alone or together with 45-kb or 88-kb plasmids. Additionally, the 45-kb plasmid also displayed *repA* hybridization signal when harbored alone. Moreover, the 120-kb plasmid present in Pss from P2 showed hybridization with the *repA* gene probe. However, this hybridization was not detected in the 120-kb plasmids present in Pss strains from P1. Interestingly, the Pss strain UMAF0292 of P2 showed *repA* hybridization signal in the 45-kb and 120-kb plasmids. Southern blot hybridization with the *rulA* gene probe exhibited results similar to those for the *repA* hybridization experiments, showing only a difference in the 62- to 88-kb plasmid profile, where both plasmids displayed *rulA* hybridization signal. However, the hybridization signal was weaker in the 88-kb plasmid. The specific plasmid profiles of each Pss strain from both populations and Southern blot analysis of *repA* and *rulA* genes are summarized in Table S1.

The distribution of 62-kb PFP copper-resistant plasmids was maintained over time. Copper resistance genes in Pss strains isolated from mango were previously reported to be mainly encoded by 62-kb plasmids (15). The number of copper-resistant strains was determined in the P1 and P2 Pss populations. Twenty-five Pss strains from P1 (66%) and 30 Pss strains from P2 (68%) could grow on 0.8 mM copper sulfate, showing that copper resistance was maintained at similar levels between P1 and P2 populations. Moreover, the MIC values for copper sulfate showed that the copper resistance level was heterogeneous, with Pss strains showing MIC values ranging from 1.0 to

TABLE 1 *Pseudomonas syringae* strains used in this study

P. syringae strain	Geographical origin	Host of isolation	Yr of isolation	Reference or source
P. syringae pv. syringae strains				
P1 population[a]				
DAR77787	Dandaragan, Australia	Mango	2007	60
DAR77789	Perth, Australia	Mango	2007	60
ICMP14923	Sicily, Italy	Mango	2002	10
ICMP14925	Sicily, Italy	Mango	2002	61
Ps10	Bet Dagan, Israel	Mango	1999	50
Ps35	Bet Dagan, Israel	Mango	1999	50
UMAF0005	Algarrobo, Málaga, Spain	Mango	1990	29
UMAF0048	Algarrobo, Málaga, Spain	Mango	1992	50
UMAF0049	Algarrobo, Málaga, Spain	Mango	1992	15
UMAF0081	Algarrobo, Málaga, Spain	Mango	1992	15
UMAF0100	Algarrobo, Málaga, Spain	Mango	1990	50
UMAF0114	Algarrobo, Málaga, Spain	Mango	1991	50
UMAF0115	Algarrobo, Málaga, Spain	Mango	1991	50
UMAF0119	Algarrobo, Málaga, Spain	Mango	1991	29
UMAF0158	Algarrobo, Málaga, Spain	Mango	1993	15
UMAF0167	Torrox, Málaga, Spain	Mango	1994	50
UMAF0170	Estepona, Málaga, Spain	Mango	1993	15
UMAF0171	Estepona, Málaga, Spain	Mango	1993	50
UMAF0174	Benajarafe, Málaga, Spain	Mango	1994	15
UMAF0176	Benajarafe, Málaga, Spain	Mango	1994	50
UMAF0185	Churriana, Málaga, Spain	Mango	1997	16
UMAF0186	Benamocarra, Málaga, Spain	Mango	2003	10
UMAF0209	Benamocarra, Málaga, Spain	Mango	2006	51
UMAF1003	Lepe, Huelva, Spain	Mango	1997	50
UMAF1029	Lepe, Huelva, Spain	Mango	1997	15
UMAF1051	Lepe, Huelva, Spain	Mango	1997	50
UMAF1065	La Redondela, Huelva, Spain	Mango	1997	50
UMAF1094	Lepe, Huelva, Spain	Mango	1998	15
UMAF1110	La Redondela, Huelva, Spain	Mango	1998	15
UMAF1128	La Redondela, Huelva, Spain	Mango	1998	15
UMAF1559.1	La Redondela, Huelva, Spain	Mango	1996	50
UMAF2007	Almansil, Portugal	Mango	1997	50
UMAF2016	Faro, Portugal	Mango	1997	15
UMAF2025	Almansil, Portugal	Mango	1998	15
UMAF2026	Almansil, Portugal	Mango	1998	15
UMAF2801	La Palma, Canary Islands, Spain	Mango	2000	61
UMAF2802	La Palma, Canary Islands, Spain	Mango	2000	50
UMAF3028[c]	Algarrobo, Málaga, Spain	Mango	1990	50
P2 population[b]				
PSM 22	Sicily, Italy	Mango	2014	62
PSM 47	Sicily, Italy	Mango	2010	62
UMAF0269	Algarrobo, Málaga, Spain	Mango	2016	This study
UMAF0271	Algarrobo, Málaga, Spain	Mango	2016	This study
UMAF0272	Algarrobo, Málaga, Spain	Mango	2016	This study
UMAF0273	Algarrobo, Málaga, Spain	Mango	2016	This study
UMAF0274	Algarrobo, Málaga, Spain	Mango	2016	This study
UMAF0275	Benamocarra, Málaga, Spain	Mango	2016	This study
UMAF0277	Torrox, Málaga, Spain	Mango	2016	This study
UMAF0278	Torrox, Málaga, Spain	Mango	2016	This study
UMAF0280	Cajiz, Málaga, Spain	Mango	2016	This study
UMAF0281	Cajiz, Málaga, Spain	Mango	2016	This study
UMAF0282	Algarrobo, Málaga, Spain	Mango	2017	This study
UMAF0283	Algarrobo, Málaga, Spain	Mango	2017	This study
UMAF0284	Algarrobo, Málaga, Spain	Mango	2017	This study
UMAF0286	Benamocarra, Málaga, Spain	Mango	2017	This study
UMAF0287	Benamocarra, Málaga, Spain	Mango	2017	This study
UMAF0288	Benamocarra, Málaga, Spain	Mango	2017	This study
UMAF0289	Benamocarra, Málaga, Spain	Mango	2017	This study
UMAF0290	Benamocarra, Málaga, Spain	Mango	2017	This study
UMAF0291[c]	Benajarafe, Málaga, Spain	Mango	2017	This study

(Continued on next page)

TABLE 1 (Continued)

P. syringae strain	Geographical origin	Host of isolation	Yr of isolation	Reference or source
UMAF0292	Benajarafe, Málaga, Spain	Mango	2017	This study
UMAF0295	Torrox, Málaga, Spain	Mango	2017	This study
UMAF0296	Torrox, Málaga, Spain	Mango	2017	This study
UMAF0297	Torrox, Málaga, Spain	Mango	2017	This study
UMAF0298	Torrox, Málaga, Spain	Mango	2017	This study
UMAF0299	Casarabonela, Málaga, Spain	Mango	2017	This study
UMAF1013	Lepe, Huelva, Spain	Mango	2017	This study
UMAF2043	Faro, Portugal	Mango	2017	This study
UMAF2044	Faro, Portugal	Mango	2017	This study
UMAF2045	Lagos, Portugal	Mango	2017	This study
UMAF2046	Lagos, Portugal	Mango	2017	This study
UMAF2047	Albufeira, Portugal	Mango	2017	This study
UMAF2048	Albufeira, Portugal	Mango	2017	This study
UMAF2600	Perth, Australia	Mango	2016	This study
UMAF2815	La Palma, Canary Islands, Spain	Mango	2016	This study
UMAF2816	La Palma, Canary Islands, Spain	Mango	2016	This study
UMAF2906	Almuñecar, Granada, Spain	Mango	2016	This study
UMAF2907	Almuñecar, Granada, Spain	Mango	2016	This study
UMAF2908	Motril, Granada, Spain	Mango	2017	This study
UMAF2909	Motril, Granada, Spain	Mango	2017	This study
UMAF2910	Almuñecar, Granada, Spain	Mango	2017	This study
UMAF2911	Almuñecar, Granada, Spain	Mango	2017	This study
UMAF5017	Níjar, Almería, Spain	Mango	2017	This study
Controls				
P. syringae pv. aptata DSM50252	USA	Sugar beet		63
P. syringae pv. avellanae ISPaVe011	Italy	Hazelnut	1992	54
P. syringae pv. japonica MAFF301072	Japan	Barley		63
P. syringae pv. phaseolicola 1448A	Ethiopia	Bean	1985	64
P. syringae pv. pisi 1704B	France	Pea	1986	63
P. syringae pv. syringae B728a	USA	Bean		65
P. syringae pv. tomato DC3000	UK	Tomato	1986	66
P. syringae pv. tomato PT23		Tomato		53
External controls of P1 and P2 populations				
EPSMV3	Gerona, Spain	Pear	1990	50
EPS17A	Gerona, Spain	Pear	1987	50
UMAF1444-5	Madrid. Spain	Laurel	1995	50
UMAF4002	Algarrobo, Málaga, Spain	Tomato	1994	50
UMAF6016	Torrijos, Málaga, Spain	Chestnut	1994	50
UMAF6024	Málaga, Spain	Purple phlomis	1995	51
UMAF6032	Algarrobo, Málaga, Spain	Melon	2016	This study
UMAF6034	Alfarnate, Málaga, Spain	Chestnut	2017	This study
UMAF6582	Periana, Málaga, Spain	Peach	1994	50
UMAF7000	Gerona, Spain	Pear	2017	This study
P. syringae pv. syringae transformant strains[d]				
UMAF0158pBBR1MCS-5				This study
UMAF0158pBBR1*cus*				This study
UMAF0158pBBR1*cop*				This study

[a]*P. syringae* pv. syringae strains isolated from mango mainly before the year 2000.
[b]*P. syringae* pv. syringae strains isolated from mango in 2016 to 2017.
[c]Pss strains names in boldface were selected for genome sequencing.
[d]Relevant characteristics for the Pss transformant strains were the following: UMAF0158pBBR1MCS-5, UMAF0158 transformed with the empty pBBR1MCS-5 vector; UMAF0158pBBR1*cus*, UMAF0158 transformed with pBBR1MCS-5*cusCBA*; UMAF0158pBBR1*cop*, UMAF0158 transformed with pBBR1MCS-5*copABmbpCDF*.

3.0 mM in P1 and from 1.0 to 2.8 mM in P2 (Table 2). Plasmid profile analysis revealed that from the 25 copper-resistant Pss strains from P1, 14 harbored at least a 62-kb plasmid. PCR with specific primers for copper resistance genes and Southern blot hybridization revealed that in 12 out of the 14 copper-resistant strains that harbored a 62-kb plasmid, the copper resistance genes were detected in the 62-kb plasmid. For P2, 18 of the 30 copper-resistant Pss strains harbored at least a 62-kb plasmid. However, the

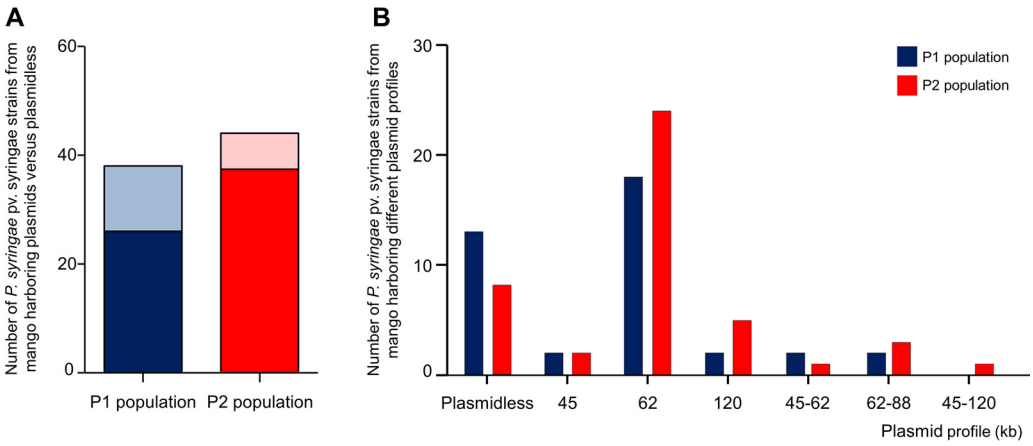

FIG 1 Plasmid content and plasmid profile distribution in *P. syringae* pv. syringae strains isolated from mango. (A) Number of *P. syringae* pv. syringae strains harboring plasmids versus plasmidless strains of P1 and P2 populations. Dark blue and light blue colors represent the number of strains belonging to the P1 population that harbor plasmids versus plasmidless strains, respectively. Dark red and light red colors represent the same data describe above but for the P2 population. (B) Number of *P. syringae* pv. syringae strains harboring different plasmid profiles. Dark blue bars represent the number of strains from P1 that harbor different plasmid profiles, and red bars represent the same data but for the P2 population.

copper resistance genes were detected in 14 out of the 18 copper resistant strains that harbored a 62-kb plasmid. Thus, copper resistance associated with 62-kb plasmids showed a similar frequency between both populations (48% and approximately 47% in P1 and P2, respectively). Additionally, 12 Pss strains from P1 and 16 Pss strains from P2 displayed different levels of copper resistance, high plasmid content variability, and no detectable copper resistance genes. In this group, it was particularly noteworthy that some Pss strains (3 from P1 and 11 from P2) showed the highest MIC values for copper sulfate of $\geq$2.4 mM (Table 2). The presence of that hyperresistant phenotype was increased in the P2 population based on Pearson chi-squared test.

Phylogenetic analysis reveals the presence of three different phylogenetic subgroups clearly associated with copper resistance phenotypes. Pss strains isolated from mango form a single phylotype inside the phylogenetic group 2 of the *P. syringae* complex, characterized by the host of isolation and the production of mangotoxin (6, 10). The phylogenetic distribution analysis performed in this study by using partial sequences of *gyrB* and *rpoD* housekeeping genes clearly showed a main clustering comprising all the Pss strains isolated from mango from both P1 and P2 populations, including 4 Pss strains isolated from other hosts (EPS17A, UMAF7000, UMAF4002, and UMAF6032) that, interestingly, showed the ability to produce mangotoxin. Nine different phylogenetic subgroups (PSG) have been observed within the Pss mango single phylotype (Fig. 2). Interestingly, all the Pss strains belonging to the phylogenetic subgroups I, II, and VIII (PSG-I, PSG-II, and PSG-VIII) were copper resistant. In particular, PSG-II comprised 7 Pss strains from P1 and 5 Pss strains from P2. All Pss strains from this PSG harbored at least a 62-kb plasmid, which encoded the *copABCD*ns structure (Table 2 and Fig. S2), showing similar MIC values for copper sulfate (between 1.8 and 2.0 mM). Intriguingly, the PSG-I subgroup clustered together 14 Pss strains and was composed predominantly of Pss strains from the P2 population (11 Pss strains). It is important to highlight that this group was composed of the Pss strains that showed the highest MIC values of copper sulfate, noted earlier (MIC, $\geq$2.4 mM copper sulfate) (Table 2). However, the genetic markers associated with this highly resistant phenotype could not be detected by PCR or by Southern blot approaches using the specific primers to detect the *copABCD* and *copABCD*ns structures. Moreover, these Pss strains have shown high plasmid content variability, although the presence of a 120-kb PFP plasmid was only found in 5 Pss strains from P2 belonging to this PSG (Table 2 and Table S1). In addition, PSG-VIII was composed of 5 Pss strains belonging to both populations that harbored different copper resistance structures (Fig. S2). The

TABLE 2 Plasmid profiles, MIC values for copper sulfate, and detection of different copper resistance determinants by PCR amplification and Southern blot hybridization in *P. syringae* pv. syringae strains isolated from mango

			PCR amplification[e]		Southern blot hybridization	
Pss strain	Plasmid profile	MIC (mM)	*copABCD*[a]	*copABCD*ns[b]	*copA*[c]	*cusA*[d]
P1 population						
DAR77787	Plasmidless	2.0	–	–	–	–
DAR77789	62	1.6	+	–	+62	–
ICMP14923	62	≤0.8	–	–	–	–
ICMP14925	Plasmidless	2.0	–	–	NT[f]	NT
Ps10	Plasmidless	1.6	–	–	–	–
Ps35	62	1.2	–	–	–	–
UMAF0005	Plasmidless	1.0	–	–	–	–
UMAF0048	62	1.8	–	+	+62	+62
UMAF0049	62–88	1.8	–	+	+62	+62
UMAF0081	62	1.8	–	+	+62	+62
UMAF0100	Plasmidless	≤0.8	–	–	–	–
UMAF0114	120	2.8	–	–	–	–
UMAF0115	Plasmidless	2.0	–	–	–	–
UMAF0119	62–88	2.0	–	+	+62	+62
UMAF0158	62	≤0.8	–	–	–	–
UMAF0167	120	2.0	–	–	–	–
UMAF0170	62	1.2	+	–	+62	–
UMAF0171	Plasmidless	≤0.8	–	–	–	–
UMAF0174	Plasmidless	≤0.8	–	–	–	–
UMAF0176	62	≤0.8	–	–	–	–
UMAF0185	62	1.8	–	+	+62	+62
UMAF0186	62	2.0	–	+	+62	+62
UMAF0209	Plasmidless	≤0.8	–	–	–	–
UMAF1003	45–62	≤0.8	–	–	–	–
UMAF1029	62	≤0.8	–	–	–	–
UMAF1051	Plasmidless	1.6	–	–	–	–
UMAF1065	62	3.0	–	–	–	–
UMAF1094	62	≤0.8	–	–	–	–
UMAF1110	62	1.6	+	–	+62	–
UMAF1128	45–62	2.0	+	–	+62	–
UMAF1559.1	62	≤0.8	–	–	–	–
UMAF2007	62	2	–	+	+62	+62
UMAF2016	62	1.8	–	+	+62	+62
UMAF2025	Plasmidless	2.0	–	–	–	–
UMAF2026	45	2.0	+	–	+45	–
UMAF2801	Plasmidless	≤0.8	–	–	–	–
UMAF2802	Plasmidless	≤0.8	–	–	–	–
UMAF3028	45	2.6	–	–	–	–
P2 population						
PSM 22	Plasmidless	≤0.8	–	–	–	–
PSM 47	62	1.8	–	+	+62	+62
UMAF0269	Plasmidless	2.4	–	–	–	–
UMAF0271	62–88	2.0	–	+	+62	+62
UMAF0272	62	1.8	–	+	+62	+62
UMAF0273	62	≤0.8	–	–	–	–
UMAF0274	62	≤0.8	–	–	–	–
UMAF0275	62	1.2	–	–	NT	NT
UMAF0277	62	1.0	+	–	+62	–
UMAF0278	62	≤0.8	–	–	–	–
UMAF0280	62	1.0	+	–	+62	–
UMAF0281	45–62	≤0.8	–	–	–	–
UMAF0282	Plasmidless	2.6	–	–	–	–
UMAF0283	62	≤0.8	–	–	–	–
UMAF0284	45	2.4	–	–	–	–
UMAF0286	62	1.2	–	–	–	–
UMAF0287	62	1.6	+	–	+62	–
UMAF0288	120	2.8	–	–	–	–

(Continued on next page)

TABLE 2 (Continued)

Pss strain	Plasmid profile	MIC (mM)	PCR amplification[e]		Southern blot hybridization	
			copABCD[a]	*copABCD*ns[b]	*copA*[c]	*cusA*[d]
UMAF0289	62	1.6	+	–	+62	–
UMAF0290	62	1.8	–	+	+62	+62
UMAF0291	45	2.8	–	–	–	–
UMAF0292	45–120	2.8	–	–	–	–
UMAF0295	Plasmidless	≤0.8	–	–	–	–
UMAF0296	120	2.8	–	–	–	–
UMAF0297	62	≤0.8	–	–	–	–
UMAF0298	120	2.6	–	–	–	–
UMAF0299	120	2.8	–	–	–	–
UMAF1013	62	2.0	+	–	+62	–
UMAF2043	120	2.4	–	–	–	–
UMAF2044	62	2.4	–	–	–	–
UMAF2045	62	2.0	+	–	+62	–
UMAF2046	62	1.6	–	–	–	–
UMAF2047	Plasmidless	1.0	–	–	–	–
UMAF2048	Plasmidless	1.6	–	–	–	–
UMAF2600	62	1.6	+	–	+62	–
UMAF2815	Plasmidless	≤0.8	–	–	–	–
UMAF2816	Plasmidless	≤0.8	–	–	–	–
UMAF2906	62	≤0.8	–	–	–	–
UMAF2907	62	1.6	+	–	+62	–
UMAF2908	62–88	1.8	–	+	+62	+62
UMAF2909	62–88	1.8	–	+	+62	+62
UMAF2910	62	≤0.8	–	–	–	–
UMAF2911	62	≤0.8	–	–	–	–
UMAF5017	62	≤0.8	–	–	–	–

[a]*copA* amplification from the typical *copABCD* operon obtained from Pss UMAF0170 62-kb PFP plasmid.
[b]*copA*, *cusA*, and *copG* amplification from the *copABCD*ns structure obtained from Pss UMAF0081 62-kb PFP plasmid.
[c]Southern blot hybridization using a *copA* probe that binds both *copA* genes from different structures.
[d]Southern blot hybridization using a *cusA* probe that binds the *cusA* gene from the *copABCD*ns structure.
[e]Plus signs indicate positive results of PCR amplifications.
[f]NT, not tested.

remaining 24 Pss copper-resistant strains were randomly distributed among the different PSGs.

Detection of a novel Tn*7*-like transposon by genome sequencing and mining. The Pss UMAF3028 strain from P1 (isolated in 1990) and Pss UMAF0291 strain from P2 (isolated in 2017), which belonged to the PSG-I and showed the same plasmid profile (45 kb), were selected to obtain their draft genome sequences. The main features of the draft genome sequences of both strains are summarized in Table S2. Bioinformatic mining of copper resistance genes was performed against the draft genome sequences of both sequenced strains using the *copABCD* and *copABCD*ns structures from the 62-kb plasmids of Pss UMAF0170 and Pss UMAF0081, respectively. By using discontiguous MegaBLAST with both copper structures, a region that could be involved in copper resistance was detected in scaffold 8.1 of both strains. In addition, the draft genome sequences of both strains were compared with the complete genome sequence of the copper-sensitive strain Pss UMAF0158 by MAUVE alignment (Fig. S3), revealing the presence of a DNA region of 51.1 kb in both strains that was not present in the copper-sensitive one. In addition, based on genome annotation, a large structure of 51,178 bp was detected in the typical attachment site for Tn*7* transposons, *att*Tn*7*, which was allocated in the chromosome downstream of the *glmS* gene of both sequenced Pss strains. The Tn*7*-like regions of Pss UMAF3028 and Pss UMAF0291 showed 100% identity between them.

The complete genetic structure of this transposon is represented in Fig. 3. The putative Tn*7*-like transposon comprised 49 open reading frames (ORFs) (Fig. 3A), which encoded several genes that could be involved in DNA repair mechanisms related to copper and arsenic resistance phenotypes (Fig. 3B and C), the typical *tnsABCDE* genes

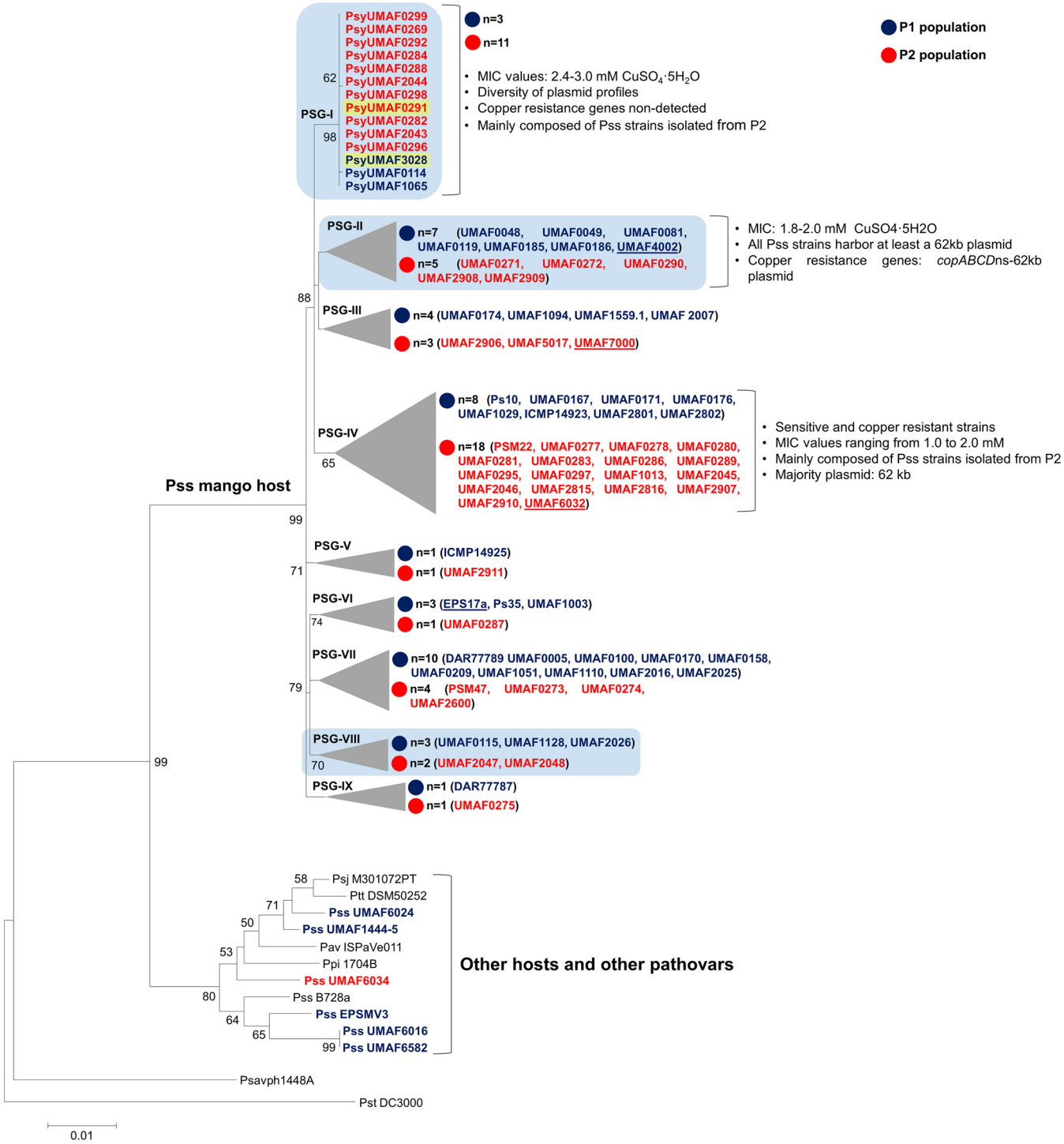

FIG 2 Phylogenetic analysis of *P. syringae* pv. syringae strains isolated from mango. The neighbor-joining tree was constructed with combined partial sequences of *gyrB* and *rpoD* housekeeping genes using MEGAv7. Bootstrap values (100 repetitions) are shown on branches, and evolutionary distances are in units of nucleotide substitutions per site. Nine different phylogenetic subgroups (PSG) are present in *P. syringae* pv. syringae strains isolated from mango and are represented in Roman numerals. Blue color shows the strains belonging to the P1 population. Red color represents the strains belonging to the P2 population. *P. syringae* pv. syringae strains isolated from other hosts but included in different subgroups of the Pss single mango phylotype are underlined (PSG-II, UMAF4002 strain isolated from tomato; PSG-III, UMAF7000 strain isolated from pear; PSG-IV, UMAF6032 strain isolated from melon; PSG-VI, EPS17A strain isolated from pear). PSG-I, PSG-II, and PSG-VIII, marked with light blue boxes, are PSGs where all Pss strains were copper resistant. Pss strains (UMAF3028 and UMAF0291) that belong to PSG-I and that are marked with yellow boxes were the strains selected for genome sequencing. Pav, *P. syringae* pv. avellanae, Pph, *P. syringae* pv. phaseolicola; Ppi, *P. syringae* pv. pisi; Psj, *P. syringae* pv. japonica; Pss, *P. syringae* pv. syringae; Pst, *P. syringae* pv. tomato; Ptt, *P. syringae* pv. aptata.

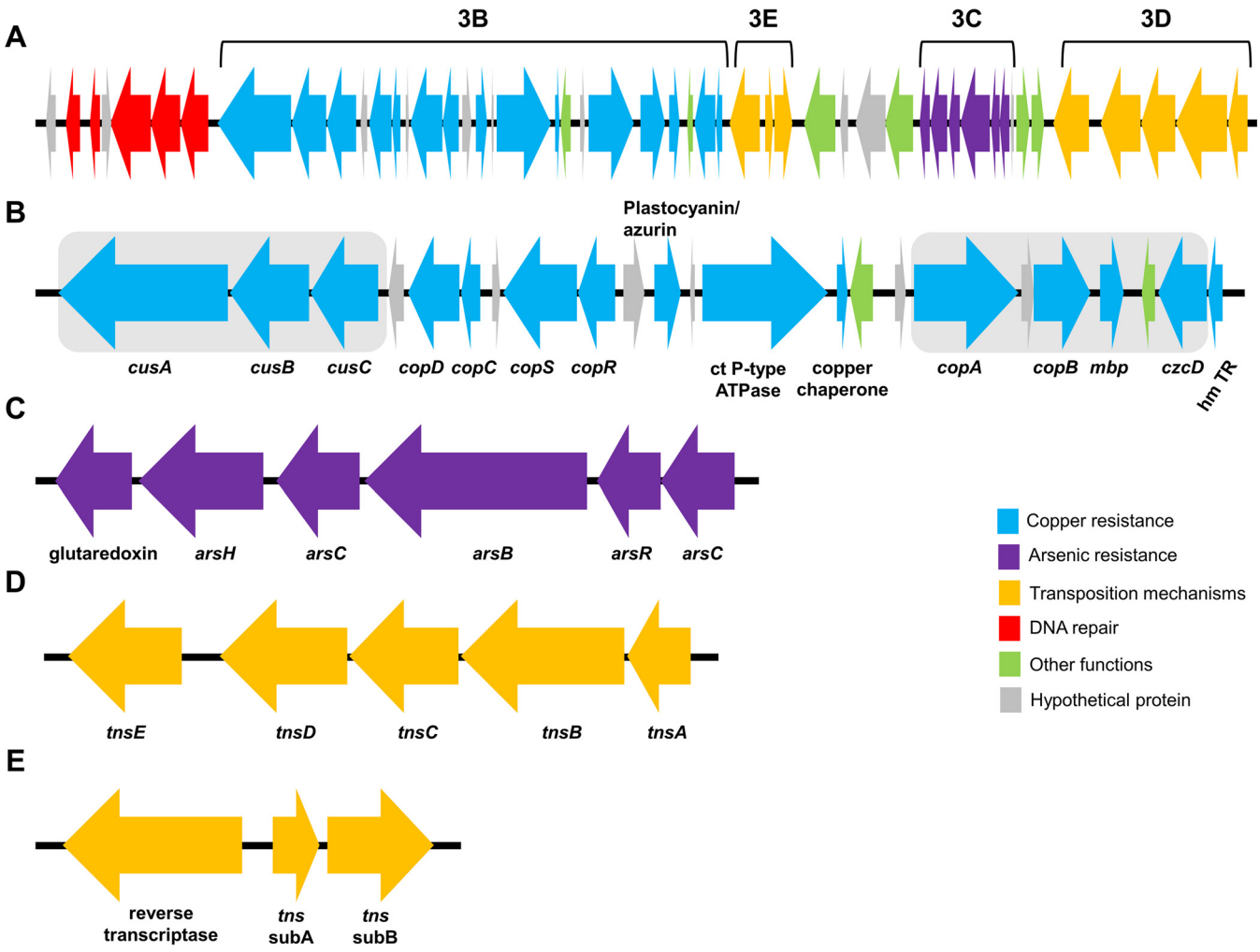

FIG 3 Genetic organization of the Tn*7*-like transposon associated with hyperresistant phenotype to copper in *P. syringae* pv. syringae strain UMAF0291. (A) Complete genetic structure of the Tn*7*-like transposon of 51,178 bp that is composed of 49 open reading frames. Gray arrows represent hypothetical proteins; red arrows represent genes putatively involved in DNA repair mechanisms; blue arrows represent genes putatively involved in copper resistance; green arrows represent genes involved in different functions; yellow arrows represent genes putatively involved in transposition mechanisms; and purple arrows represent genes putatively related to detoxification of arsenic compounds. (B) Genetic structure related to copper resistance, composed of 23 open reading frames. (C) Genetic structure of genes related to arsenic resistance, composed of six open reading frames. (D) Genetic structure of the typical transposition machinery of Tn*7* transposons encoded by *tnsABCDE* genes. (E) Genetic structure of a retrotransposon. Gray boxes represent the DNA fragments cloned into pBBR1MCS-5 vector.

that form the transposition mechanism of Tn*7* transposons (Fig. 3D), and a retrotransposon (Fig. 3E). Putative specific functions of the ORFs predicted in the Tn*7*-like transposon are summarized in Table S3. This Tn*7* transposon was designated COARS Tn*7*-like due to its putative ability to detoxify copper and arsenic compounds. In addition, all Pss strains from mango from both populations were interrogated for the presence of the COARS Tn*7*-like transposon based on PCR amplification of *copA* and *cusA* genes from the Tn*7* structure. Only those Pss strains from PSG-I apparently contained the COARS Tn*7*-like transposon (Fig. S2). A nucleotide BLAST search of this Tn*7* region was performed and revealed that this Tn*7*-like transposon was present, with some differences, in the genome of some soil and water strains belonging to the *Pseudomonas fluorescens* complex and in two strains of *P. syringae* pv. actinidiae (Psa NZ-64 and Psa SR121). A comparative genetic map among the Tn*7*-like transposons present in Pss UMAF0291, Psa SR121, and *P. rhodesiae* BS2777 strains is represented in Fig. S4.

COARS Tn*7*-like transposon confers hyperresistant phenotype to copper in *P. syringae* pv. syringae strains isolated from mango. To decipher the role of the COARS Tn*7*-like transposon in the detoxification of copper sulfate, transformant strains

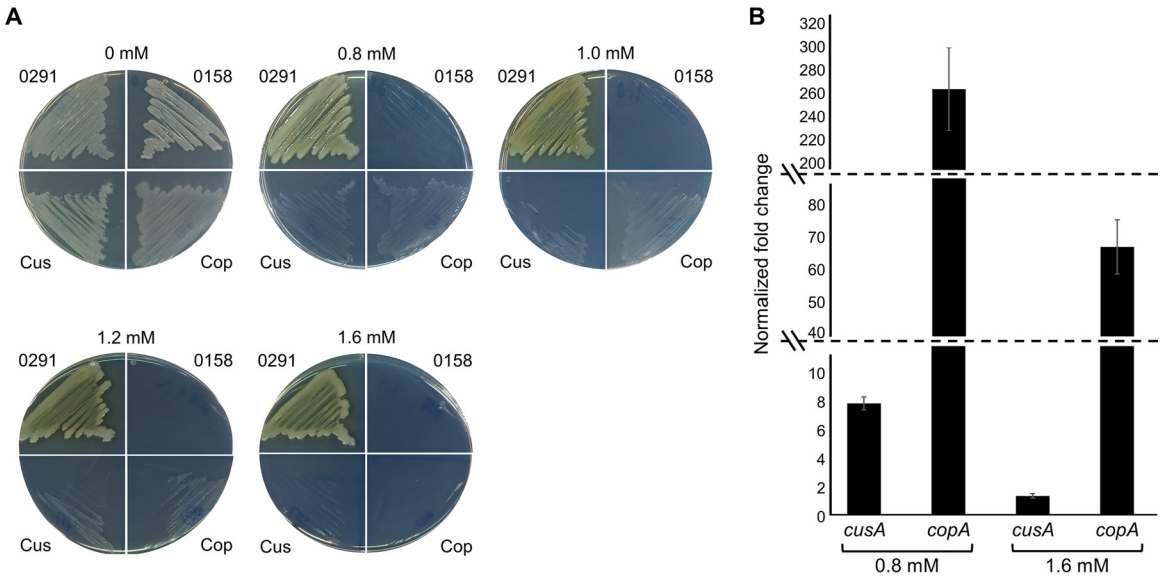

FIG 4 Transformation and RT-qPCR experiments on selected putative copper resistance genes. (A) MICs of copper sulfate in MGY medium supplemented with different concentrations of copper sulfate (0.8 mM, 1.0 mM, 1.2 mM, and 1.6 mM). The transformants of the copper-sensitive *P. syringae* pv. syringae UMAF0158 (Pss UMAF0158) strain that harbor the *cusCBA* (Cus) genes and *copAB*, a metal binding protein and a CDF transporter (Cop) gene, were tested. The Pss UMAF0158 copper-sensitive strain and Pss UMAF0291 copper-resistant strain that harbors the Tn*7*-like transposon are included as negative and positive controls, respectively. (B) RT-qPCR experiments were performed on the Pss UMAF0291 copper resistance strain on two putative copper resistance genes. One of each is present in each construction describe above (*cusA* and *copA*). The results are shown as the fold change in expression of *cusA* and *copA* genes at 0.8 and 1.6 mM copper sulfate compared with the control condition (absence of copper).

derived from the copper-sensitive strain Pss UMAF0158 were generated, including two different regions that harbored putative genes involved in copper resistance from the COARS Tn*7*-like transposon of the Pss UMAF0291 strain. The transformant strain Pss UMAF0158pBBR1*cus*, which harbored the *cusCBA* operon, increased the MIC to 1.0 mM copper sulfate. The second transformant, Pss UMAF0158pBBR1*cop*, which harbored the genes *copAB*, a metal binding protein and a CDF transporter, showed a MIC of 1.2 mM copper sulfate (Fig. 4A). Thus, both transformants provided a copper-resistant phenotype to the Pss UMAF0158 sensitive strain. In addition, reverse transcription-quantitative PCR (RT-qPCR) experiments were performed on the putative copper resistance genes *copA* and *cusA* present in the COARS Tn*7*-like transposon from Pss UMAF0291. The expression of both genes was strongly increased at the two different concentrations of copper tested (0.8 and 1.6 mM) compared with their expression in the absence of copper sulfate (Fig. 4B). Compared with the control condition (0 mM copper sulfate), the *copA* gene showed an overexpression of 269- and 69-fold changes at 0.8 mM and 1.6 mM copper sulfate, respectively. Additionally, the *cusA* gene showed an overexpression with respect to the control condition of 7.7-fold change at 0.8 mM copper sulfate. However, its relative expression at 1.6 mM with respect to the control condition was not increased (Fig. 4B).

DISCUSSION

Copper-based compounds have been widely used since the middle of the 18th century in agriculture as standard bactericides to control plant diseases (11). Pss is a phytopathogenic bacterium distinguished from other pathovars of the *P. syringae* complex due to its ability to infect a large variety of woody and herbaceous plants (31). Pss has been identified as the causal agent of BAN disease in mango trees (8). The copper-based spray compound Bordeaux mixture (BM) has been used as the conventional treatment to control BAN disease caused by Pss (32, 33). Nevertheless, the continuous use of copper by growers has served as a selection pressure mechanism that has sharply increased the number of copper-resistant bacterial phytopathogens, including

P. syringae, and improved the evolution of copper resistance determinants, which are mainly allocated in plasmids (15, 18, 19, 30, 34). Therefore, in this study, two different Pss populations isolated from mango from the same worldwide region (mainly from southern Spain) and that were isolated with an average of 20 years of difference were assessed to better understand the evolution of copper resistance and their specific detoxification mechanisms through time in a particular host and environment.

Plasmids that are part of what is known as a flexible genome are one of the main drivers of bacterial evolution (21, 24). The PFP family of plasmids is widely distributed among pathovars of *P. syringae* and related species of the *P. syringae* complex (24, 26, 35). The presence of 62-kb plasmids belonging to the PFP family has been described in Pss strains isolated from mango (15, 26). To characterize the plasmids harbored in both Pss populations analyzed in this study, the presence of the *repA* gene was assessed (24, 26, 35). Our results confirmed previous data that suggested nearly all 62-kb plasmids present in Pss from mango belonged to the PFP family (10, 15). Furthermore, the presence of plasmids that do not belong to the PFP family (non-PFP) has been widely described in *P. savastanoi* pv. savastanoi, a related phytopathogenic bacterium, displaying an important contribution to virulence and fitness (36).

PFP plasmids do not encode basic survival functions of their bacterial hosts but contribute to their virulence and ecological fitness (15, 24, 25, 37–40). Some of the most relevant accessory determinants carried by PFPs are copper resistance and UV radiation resistance genes (39, 41, 42).The *rulAB* genes have been found to be tightly associated with the 62-kb PFP plasmids in Pss from mango, improving their tolerance to UV radiation (29). Interestingly, the *rulA* gene was also detected in the 88-kb non-PFP plasmid, which suggests the Pss strains with the 62- to 88-kb plasmid profile has a significant advantage in surviving on the mango plant surface.

The total content of plasmids was found at similar levels over time. Our findings also highlighted that the 62-kb PFP plasmid profile was also maintained at similar levels between both Pss populations. Copper resistance determinants are also important accessory genes carried by PFP plasmids that confer an important ecological fitness advantage (24, 26, 37) and have been described in Pss strains isolated from mango mainly carried by 62-kb PFP plasmids (15). Two different copper resistance determinants have been reported in 62-kb PFP plasmids, the typical *copABCD* operon and the novel gene cluster *copABCD*ns, both being structures relevant to the survival of Pss under exposure to copper treatments (15, 26, 30). In previous works, copper resistance was found at similar levels in Pss from mango but mostly associated with 62-kb plasmids (10, 15). Likewise, our results have shown that copper resistance was maintained over time, showing similar levels between P1 and P2 populations. These results could point out that some mechanisms of selection pressure, among which copper could be one of the most relevant, act by maintaining the plasmid content over time, mostly 62-kb PFP copper-resistant plasmids, which display an important role in the epiphytic lifestyle of Pss (15, 26). Moreover, there were some Pss strains (12 from P1 and 16 from P2) that displayed a copper-resistant phenotype and showed no homology with any of the copper resistance determinants described previously. This fact suggests that novel copper resistance determinants are present in Pss mango populations. Curiously, among these Pss copper-resistant strains, there was an increase over time of a hyperresistant phenotype to copper, with MIC values of $\geq$2.4 mM (3 Pss strains from P1 and 11 Pss strains from P2).

The phylogenetic analysis performed in this study revealed that within this single mango phylotype (10), at least nine different PSGs were detected. It is noteworthy that three of them showed a strong correlation with the copper-resistant phenotype, PSG-I, PSG-II, and PSG-VIII. Outstandingly, all Pss strains that showed the highest MIC values for copper sulfate were phylogenetically clustered within the PSG-I. As far as we know, this particular phylogenetic copper phenotype association has not been clearly observed in any other bacteria, with the exception of the nosocomial pathogen *Enterococcus faecium* (43).

By genome sequencing and mining, a Tn*7*-like transposon that encoded putative genes involved in copper and arsenic resistance was found. Copper and arsenic resistance modules have been previously reported clustering and associated with mobile genetic elements (26). Genes involved in antibiotic resistance and pathogenesis and others involved in adaptive mechanisms have been frequently found in Tn*7* transposons (44). In addition, Tn*7*-like transposons have been found in a wide range of bacteria belonging to the *Firmicutes*, *Cyanobacteria*, *Bacteroidetes*, and *Proteobacteria* phyla (44). These types of transposons carry the *tnsABCDE* genes, which form the transposition machinery. In our case, the transposon designated COARS Tn*7*-like was found to be located at the *att*Tn*7* site located downstream of the *glmS* gene on the chromosome and carried the *tnsABCDE* genes, similar to what has been observed previously (45, 46). Similar genetic structures of the COARS Tn*7*-like transposon have been observed in the genomes of some *Pseudomonas* species belonging to the *P. fluorescens* complex and in Psa (19). It is worth highlighting that this Tn*7* transposon in Psa is inserted at a different location in the chromosome, as it is an integrative conjugative element (ICE), and that the MIC for copper sulfate (1.2 mM) was lower than that with the COARS Tn*7*-like transposon (≥2.4 mM). The ICE location could provide an advantage to be horizontally transferred, spreading the structure to other bacteria. However, the COARS Tn*7*-like transposon at the typical *att*Tn*7* site could offer a higher copper resistance. Different approaches to demonstrate the transfer of COARS Tn*7*-like or to prove the involvement in copper resistance of some of its genes by insertional or deletion mutagenesis failed. Thus, to link genomic information with functionality, some genes putatively relevant for copper resistance were cloned and expressed in a Pss copper-sensitive strain, proving the role of these genes in copper resistance. RT-qPCR experiments also supported these findings. The differences in the relative expression of the different genes tested suggested that a dynamic response against different concentrations of copper exists in the COARS Tn*7*-like transposon. Hence, the role of the COARS-Tn*7*-like transposon in copper resistance in Pss strains isolated from mango was demonstrated. These results suggest that a novel copper resistance determinant that provides higher resistance could have been selected instead of other copper resistance determinants in Pss mango populations over time, probably favored by continuous copper exposure.

Overall, in this study it has become evident that copper resistance and plasmid content, in particular the 62-kb PFP copper-resistant plasmids, were maintained at similar levels over time in spite of continuous applications of copper. Interestingly, a new copper resistance determinant, with a much more complex structure based on the Tn*7*-like transposon of chromosomal location that provides higher copper detoxification, has been selected and increased over time. Finally, understanding in depth the evolution of copper resistance in plant-pathogenic bacteria could shed light on the design of more efficient control programs through the rational application of copper.

MATERIALS AND METHODS

Bacterial strains and growth conditions. Eighty-two Pss strains isolated from mango from different worldwide regions, but mainly from southern Spain, and separated in time by an average of 20 years were used in this study. This Pss collection was composed of two populations, designated P1 and P2. The P1 population ($n = 38$) comprised Pss strains randomly selected from our research group collection and were mainly isolated before the year 2000. In addition, seven Pss strains isolated from other hosts, including pear ($n = 2$; EPSMV3 and EPS17A), laurel (UMAF1444 and UMAF1445), tomato (UMAF4002), chestnut (UMAF6016), purple phlomis (UMAF6024), and peach (UMAF6582), were included as external controls of the P1 population. The P2 population ($n = 44$) comprised Pss strains isolated during the years 2016 and 2017. Three Pss strains isolated from other hosts, including melon (Pss UMAF6032), chestnut (Pss UMAF6034), and pear (Pss UMAF7000), also were included as external controls of the P2 population. In addition, eight strains of *P. syringae* belonging to seven different pathovars, such as pv. aptata ($n = 1$), pv. avellanae ($n = 1$), pv. japonica ($n = 1$), pv. phaseolicola ($n = 1$), pv. pisi ($n = 1$), pv. syringae ($n = 1$), and pv. tomato ($n = 2$), were used as control strains in the different experimental approaches performed in this study. All strains were cultured routinely in King's B (KB) agar and lysogeny broth (LB) media and incubated at 25°C for 24 h. All strains used in this work are summarized in Table 1.

Bacterial isolation and identification. To generate the P2 population, bacterial isolation during the years 2016 and 2017 was performed according to the following procedure. Small pieces of symptomatic

mango tissues were collected from the field, preferentially from apical buds but also from petioles and leaves, from the same or the nearest mango growing areas as those of the isolates belonging to the P1 population. The samples were processed by two approaches: (i) small portions of samples were surface disinfected by immersion in a sterile aqueous solution of sodium hypochlorite (10%), 96% ethanol (10%), and sterile distilled water (80%) for 2 min, two wash steps of 2 min in sterile distilled water, and then plated on KB agar medium plates supplemented with cycloheximide (100 μg/ml) to prevent fungal growth, and (ii) small portions of samples were placed in sterile plastic bags, and 10 ml of sterile phosphate buffer (10 mM, pH 7.2) per gram of fresh weight was added. The samples were homogenized in a laboratory blender (Colworth Stomacher-400; Seward Ltd.) for 3 min, and the resultant suspension was used for 10-fold serial dilutions in sterile phosphate buffer. One hundred-microliter aliquots of each 10-fold serial dilution were plated onto KB agar medium amended with cycloheximide (100 μg/ml) to prevent fungal growth. Regardless of the approach, KB agar plates were incubated at 25°C for 2 to 5 days. Fluorescent colonies under UV light (265 nm) were selected and identified using different biochemical and physiological tests (8). These tests included Gram staining, glucose metabolism, LOPAT tests, with the exception of potato soft rot (levan production, cytochrome *c* oxidase reaction, arginine dihydrolase, and tobacco hypersensitivity response), hydrolysis of esculin and gelatin, and utilization of different carbon sources (glucose, mannitol, sorbitol, gluconate, propionate, L-histidine, L-lactate, L-tartrate, inositol, and adonitol). All media were incubated at 25°C for 3 to 5 days. Ice nucleation activity (INA) of bacterial isolates was detected following a tube test described previously (47). Furthermore, the bacterial isolates were interrogated for the presence by PCR amplification of the main gene, *syrB*, involved in the biosynthesis of syringomicin, a lipodepsipeptide toxin mainly associated with the pathovar syringae. The primer sequences and amplicon sizes are listed in Table 3 (48). The production of syringomicin was analyzed by using the growth inhibition test on potato dextrose agar (PDA) medium using *Geotrichum candidum* F-260 as the indicator strain (49). All tests described above were carried out at least in duplicate. All tests were also carried out in the Pss strains belonging to the P1 population to confirm all of them were identified correctly as Pss.

Mangotoxin production assay and detection of the mangotoxin biosynthetic operon (*mbo*) by PCR. The detection of the *mbo* operon and the production of mangotoxin were used in this work as markers to identify Pss strains belonging to the Pss single mango phylotype. Mangotoxin production was detected by an indicator technique based on the growth inhibition of *Escherichia coli* (50). Briefly, a double layer agar plate with *Pseudomonas* minimal medium (PMS) was prepared and solidified with the indicator strain *E. coli* CECT831. To evaluate mangotoxin activity, 100 μl of a 6 mM solution of *N*-acetyl-ornithine or L-ornithine was added to the double layer of *E. coli*. The bacterial strains to be tested then were stab-inoculated and the plates were incubated at 22°C for 24 h, with an additional incubation step of 24 h at 37°C. Mangotoxin production was detected due to the presence of growth inhibition halos. The presence of the *mbo* operon was assessed by PCR using specific primers that amplified an overlapping fragment of the *mboA* and *mboB* genes (Table 3) (51). Both approaches were performed at least in duplicate.

Plasmid profile. Plasmid DNA from the 82 *P. syringae* pv. syringae strains isolated from mango included in this study was isolated according to an alkaline lysis method (52) and separated by electrophoresis on 0.8% agarose gels. Plasmid size was estimated by comparison with the *P. syringae* pv. tomato PT23 (Pst PT23) control strain, which harbors four plasmids: pPT23A (100 kb), pPT23B (83 kb), pPT23C (65 kb), and pPT23D (36 kb) (53). Several P1 strains, previously described to harbor different plasmid profiles, were also used as controls (Pss UMAF0158 [62 kb], Pss UMAF0049 [62 kb, 88 kb], Pss UMAF1128 [45 kb, 62 kb], and Pss UMAF3028 [45 kb]). Plasmid profile analyses were performed in triplicate.

Analysis of the MIC of copper sulfate. Copper resistance was determined by using mannitol-glutamate-yeast extract agar medium (MGY). The Pss strains that could grow on all surfaces streaked on MGY supplemented with 0.8 mM copper sulfate after 72 h at 25°C were considered copper resistant. For Pss copper-resistant strains, the MICs of copper sulfate were determined. The copper sulfate concentrations tested were 0.8, 1.0, 1.2, 1.6, 2.0, 2.4, 2.8, 3.0, and 3.2 mM. Pss strains growing on MGY supplemented with the different concentrations of copper sulfate after 72 h at 25°C were considered resistant to that concentration. MIC experiments were repeated in triplicate.

PCR detection of copper resistance genes. Two different copper resistance determinants have been described in Pss strains isolated from mango: the typical *copABCD* operon and *copABCD*ns (26, 30). To differentiate the copper resistance determinants, PCR analyses were performed using specific primers that amplified fragments of the *copA* gene sequences of PssUMAF0170 and PssUMAF0081 62-kb plasmids, which harbored *copABCD* (copAF and copAR) and *copABCD*ns (copAnsF and copAnsR) structures, respectively. Specific primers were also designed on the sequences of *cusA* (cusAnsF and cusAnsR) and *copG* (copGnsF and copGnsR) genes of the *copABCD*ns structure. The primer sequences and the amplicon sizes are summarized in Table 3.

Southern blot analysis. The genomic locations of *repA*, *rulA*, *copA*, and *cusA* genes were assessed by Southern blot hybridization using plasmid DNA extractions that were separated by electrophoresis in 0.8% agarose gels. Due to the nucleotide sequence variability of the *copA* gene of the different structures, a unique primer set to amplify different *copA* gene variants was designed based on a highly conserved sequence of 4 different *copA* genes present in plasmids of different *P. syringae* strains (Pss UMAF0081, Pss UMAF0170, Pss 7B44, and Pst PT23). The DNA probes obtained from the purified PCR amplicons were labeled with digoxigenin (DIG) using a DIG-high prime labeling kit (Roche, Basel, Switzerland) by following the manufacturer's instructions. Plasmid DNA extraction gel was transferred to nylon membranes and cross-linked in a UV chamber. For membrane hybridization, a DIG Easy Hyb kit

TABLE 3 Primers used in this study for PCR, RT-qPCR, and Southern blot experiments

Primer name	Primer sequence 5′–3′	Amplicon size (bp)	Reference or source
PCR amplification			
Syringomicin			
syrB1	CTTTCCGTGGTCTTGATGAGG	752	48
syrB2	TCGATTTTGCCGTGATGAGTC		
Mangotoxin			
mbo24-For	CAAGGACGAGAAGGATCTGC	692	51
mbo24-Rev	CGACATTCAAACGACTCAGG		
copABCD			
copAF	ATGAAGATGAACCCCACGGA	435	This study
copAR	GTCCATACCACCCATGCCCA		
*copABCD*ns			
copAnsF	ATGAAGATGAACCCCACTGA	717	This study
copAnsR	GGCCTGCATGTCAACCAACG		
cusAnsF	GGATTCCATCCGAGCATCAG	492	This study
cusAnsR	TGTCGATGCGGTTGCGAATG		
copGnsF	CTGGTCATTGCCTGCCCTTG	500	This study
copGnsR	GCGCCTAGCTCGATCAACC		
Phylogeny			
rpoDfor2	ACCGATCCCGTTCGTATGTA	907	54
rpoDrev2	TGGTGTACTTCTTGGCGATG		
gyrBfor2	GTCATCATGACCGTGCTCCA	996	54
gyrBrev2	CCCTTCCACCAGGTACAGTT		
COARS Tn*7*-like			
copATn*7*F	AGATCCTAGTCGCGTCATGG	390	This study
copATn*7*R	ACGGCGATGCGGAATTCGTC		
cusATn*7*F	TCGCGTTGGTCTGCGGAATC	394	This study
cusATn*7*R	AACGCCAATGGACCGAATAG		
Copper transformants[a]			
cus-xhoIF	CC**CTCGAG**GGCCGCTCGTACAAACCTCTTC	6,086	This study
cus-xbaIR	GC**TCTAGA**GCACGGGCTGTGCAGCTCAAAC		This study
cop-apaIF	GC**GGGCCC**GCTCGCTTGCCGTAAGAGTTTG	5,597	This study
CDF-speIR	GG**ACTAGT**CCCGAAGACCACGCTCGTGAAC		This study
RT-qPCR experiments			
copATn*7*RTF	AGCGTACTCACTGGCAATGA	199	This study
copATn*7*RTR	GAATGATCCCGTGCCAATGG		This study
cusATn*7*RTF	CAACCACCATGCTCTCAGTG	194	This study
cusATn*7*RTR	AGTGGCATCAGGTCCTAAGG		This study
qRT-PCR158_gyrB_F	TGCTGACCTTCTTCTTCCGT	198	59
qRT-PCR158_gyrB_R	AGATACCTGGAGCCGATTCG		
Southern blot experiments			
Copper resistance			
copA-probeF	CCACAGCCACTCCGGATTTC	332	This study
copA-probeR	CATTGAGCAGGTACGTGTAG		
cusA-probeF	GGATTCCATCCGAGCATCAG	192	This study
cusA-probeR	ACAGCAAATCGCCTTCATCC		
Plasmid replication			
repA-probeF	TGGTGTCCTGGCTGGTGTTC	203	This study
repA-probeR	GGCAAACGCGGCATAGATCG		
Ultraviolet resistance			
rulA-probeF	CCAAGATCGATGGCGACAGC	200	This study
rulA-probeR	GATATGCCGAGGCGGATAGG		

[a]Sequences in boldface represent restriction enzyme cutting sites.

was used (Roche), and immunological detection was performed with an anti-DIG antibody conjugated to alkaline phosphatase. The DIG-labeled nucleic acids were detected by chemiluminescence using a Molecular Imager ChemiDoc system (Bio-Rad, United Kingdom). Prehybridization and hybridization were performed at low stringency (50°C) for *copA* and *cusA* and a high stringency (60°C) for *repA* and *rulA* genes. The primer sequences and the amplicon sizes to obtain DNA probes for the different genes are summarized in Table 3. Pst PT23, Pss UMAF0081 (*copABCD*ns structure in a 62-kb plasmid), PssUMAF0170 (*copABCD* in a 62-kb plasmid), and Pss UMAF0158 (copper-sensitive strain that harbors a 62-kb plasmid) were included in all gels as controls. These experiments were repeated at least in duplicate.

Phylogenetic analysis. Partial sequences of *rpoD* and *gyrB* housekeeping genes were used to analyze the phylogenetic distribution of the Pss strains that belong to the mango single phylotype compared with other *P. syringae* strains that belong to different pathovars. Some of the partial sequences from the Pss strains belonging to the P1 population and control strains were available at the NCBI database, and the rest of the partial sequences from the Pss were obtained in this study. The partial sequences of the housekeeping genes *rpoD* and *gyrB* were obtained by PCR using specific primers listed in Table 3 (54). PCR products were purified and sent for sequencing to STABvida (Portugal). The partial sequences of *rpoD* (807 bp) and *gyrB* (890 bp) were concatenated for each strain and treated as a single sequence for multiple alignments using MUSCLE (EMBL-EBI). Phylogenetic trees were generated using MEGAv7 (55) with neighbor-joining, Jukes-Cantor Model, maximum likelihood, and complete deletion to eliminate positions containing gaps. Confidence levels of the branching points were determined using 1,000 bootstrap replicates.

Genome sequencing. Pss strain UMAF3028 (isolated in 1990) and Pss strain UMAF0291 (isolated in 2017) were selected to obtain their draft genome sequences. Overnight shaking of cultures growing in LB broth tubes at 25°C of both Pss strains was used to perform total DNA isolation using the DNeasy UltraClean microbial kit (Qiagen). DNA libraries were prepared using the Nextera XT DNA library preparation kit for small genomes (Illumina, Inc., USA). The draft genome sequencing project was performed by the Supercomputing and Bioinnovation Center of the University of Málaga using the sequencing platform NextSeq550 with paired-end reads with a read length of 150 bp. The raw reads were preprocessed using SeqTrimNext software (56), and the assembly of high-quality filtered reads was performed using A5 software with default parameters (57). Genome sequence annotation and gene identification were carried out with the NCBI Prokaryotic Genome Annotation Pipeline (PGAP) using default parameters.

Bioinformatic mining for copper resistance genes. Nucleotide sequence searches to detect putative copper resistance genes were performed using nucleotide BLAST by following two approaches, highly similar sequences (MegaBLAST) and more dissimilar sequences (discontiguous MegaBLAST) against *copABDC* and *copABCD*ns gene clusters from Pss UMAF0170 and Pss UMAF0081, respectively. PGPA annotations then were used to analyze the regions that showed some similarities to identify putative copper resistance genes. Furthermore, the complete genome sequence of the Pss UMAF0158 copper-sensitive strain (58) was aligned against the draft genome sequences of Pss UMAF3028 and Pss UMAF0291 using MAUVE software with progressiveMAUVE alignment for efficient multiple genome alignment to detect gene gain, loss, and rearrangement. Specific primers were designed to PCR amplify partial sequences of putative copper resistance genes *copA* (copATn*7*F and copATn*7*R) and *cusA* (cusATn*7*F and cusATn*7*R) from the COARS Tn*7*-like transposon. Primer sequences and amplicon sizes are listed in Table 3.

Transformant strains and screening for copper resistance. To determine the functionality of some genes related to copper resistance in the COARS Tn*7*-like transposon, transformation experiments were performed. Specific primers with restriction sites for double digestion and directional ligation into the pBBR1MCS-5 vector were designed on the sequence of the COARS-Tn*7*-like transposon of the Pss UMAF0291 strain. A fragment containing *cusCBA* genes (6,086 bp) was amplified by PCR with the primers cus-xhoIF and cus-xbaIR, which harbored restriction sites for XhoI and XbaI, respectively. A second fragment containing *copAB*, a metal binding protein and a CDF transporter (5,597 bp), was also amplified by PCR with the primers cop-apaIF and CDF-speIR, which harbored restriction sites for ApaI and SpeI, respectively. Primer sequences are included in Table 3. PCR amplifications were performed using Phusion high-fidelity DNA polymerase (Thermo Fisher Scientific Inc., USA) by following the manufacturer's instructions. The PCR products were purified, double digested, cloned into pBBR1MCS-5, which harbors a gentamicin resistance gene, and transformed into electrocompetent cells of the copper-sensitive strain Pss UMAF0158. For copper resistance screening, cultures of Pss UMAF0158 transformant strains were grown overnight in LB agar medium supplemented with 15 μg/ml gentamicin (Gm) and directly streaked onto MGY agar plates supplemented with different concentrations of copper sulfate (0.6, 0.8, 1.0, 1.2, and 1.6 mM). Pss UMAF0158 was used as the negative control, and Pss UMAF0291 was used as the positive control.

RNA isolation and RT-qPCR on putative copper resistance genes. The Pss UMAF0291 strain was grown overnight in LB broth shaking cultures at 25°C. The culture was washed two times in sterile 0.85% NaCl, and 100-ml flasks with 20 ml of MGY broth without copper sulfate (0 mM) and supplemented with 0.8 mM and 1.6 mM copper sulfate were inoculated at an optical density at 600 nm of 0.1 (approximately 10^7 CFU/ml). Flasks were incubated for 6 h at 25°C, and 5 ml of each flask was collected and centrifuged at 8,000 rpm for 3 min. Total RNA was extracted using an RNA isolation kit (NucleoSpin RNA, minikit for RNA purification; Macherey-Nagel GmbH & Co. KG, Germany). The total RNA concentration was determined with a NanoDrop 2000 spectrophotometer (Thermo Fisher Scientific Inc., USA), and RNA integrity was assessed by agarose gel electrophoresis. The absence of genomic DNA contamination was tested by PCR amplification of RNA samples using specific primers that amplify the *syrB* gene (Table 3). DNA-free total RNA then was converted to cDNA using Superscript III reverse transcriptase (Invitrogen, USA) and random primers according to the manufacturer's instructions. The RT-qPCR assays were conducted in a CFX96 Touch qPCR system (Bio-Rad, USA) using SyBrGreen supermix (Bio-Rad, USA). Two independent RNA extractions for each condition and three technical replicates per extraction were assessed. Specific primers were designed using the Primer3 website (http://primer3.ut.ee/) on *cusA* and *copA* gene sequences from the COARS Tn*7*-like transposon. The housekeeping gene *gyrB* was used as the reference gene (59). Primer sequences and amplicon sizes are summarized in Table 3. The relative transcript abundance was calculated using the $\Delta\Delta C_T$ (cycle threshold) method. The expression of *cusA* and *copA* at 0 mM copper sulfate was used for the normalization of RT-qPCR at 0.8 and 1.6 mM copper sulfate.

Statistical analysis. The Pearson chi-squared test was used to evaluate the difference in plasmid content between P1 and P2 populations and, in particular, the presence of 62-kb plasmids. In addition, this statistical test was used to evaluate the number of copper hyperresistant strains and the presence of the COARS Tn*7*-like transposon between both populations. A significance level of 0.05 was applied in all cases.

Data availability. GenBank accession numbers of the different *Pseudomonas syringae* plasmids (Pss UMAF0081, Pss UMAF0170, Pss 7B44, and Pst PT23) harboring different *copA* genes were KY362368, KY362372, KY362373, and MSDS00000000, respectively. GenBank accession numbers of the partial nucleotide sequences of *rpoD* and *gyrB* genes for each bacterial strain are listed in Table S4 in the supplemental material. The partial nucleotide sequences of the *gyrB* gene obtained in this study have been deposited at GenBank under the accession numbers MW001941 to MW002005. The partial nucleotide sequences of the *rpoD* gene obtained in this study have been deposited at GenBank under the accession numbers MW002006 to MW002070. The draft genome sequences obtained in this work have been deposited at GenBank under accession numbers JACTWA000000000 and JACTWB000000000 for Pss UMAF0291 and Pss UMAF3028, respectively.

SUPPLEMENTAL MATERIAL

Supplemental material is available online only.

SUPPLEMENTAL FILE 1, PDF file, 2.6 MB.

ACKNOWLEDGMENTS

This work was supported by grants from CICE-Junta de Andalucía, Proyecto de Excelencia (P12-AGR-1473) from Junta de Andalucía, Proyecto Spanish Plan Nacional I+D+I (AGL2017-83368-C2-1-R) and cofinanced by Proyecto FEDER UMA18-FEDERJA-046. Jose A. Gutiérrez-Barranquero was supported by a postdoctoral fellowship from the Plan Propio de Investigación y Transferencia of the University of Malaga "Ayuda de Incorporación de Doctores."

We thank Irene Linares for her technical support during the development of this work. We also thank the Supercomputing and Bioinnovation Center of the University of Málaga for its technical support.

J.A.G.-B. and A.V. designed the study, F.A. and Z.H.-P. performed the experiments, and F.M.C. and J.A.G.-B. analyzed the data and drafted the manuscript.

REFERENCES

1. Baltrus DA, McCann HC, Guttman DS. 2017. Evolution, genomics and epidemiology of *Pseudomonas syringae*. Mol Plant Pathol 18:152–168. https://doi.org/10.1111/mpp.12506.
2. Arrebola E, Cazorla FM, Perez-García A, de Vicente A. 2011. Chemical and metabolic aspects of antimetabolite toxins produced by *Pseudomonas syringae* pathovars. Toxins (Basel) 3:1089–1110. https://doi.org/10.3390/toxins3091089.
3. Ichinose Y, Taguchi F, Mukaihara T. 2013. Pathogenicity and virulence factors of *Pseudomonas syringae*. J Gen Plant Pathol 79:285–296. https://doi.org/10.1007/s10327-013-0452-8.
4. Xin XF, Kvitko B, He SY. 2018. *Pseudomonas syringae*: what it takes to be a pathogen. Nat Rev Microbiol 16:316–328. https://doi.org/10.1038/nrmicro.2018.17.
5. Gardan L, Shafik H, Belouin S, Broch R, Grimont F, Grimont PA. 1999. DNA relatedness among the pathovars of *Pseudomonas syringae* and description of *Pseudomonas tremae* sp. nov. and *Pseudomonas cannabina* sp. nov. (ex Sutic and Dowson 1959). Int J Syst Bacteriol 49:469–478. https://doi.org/10.1099/00207713-49-2-469.
6. Gutiérrez-Barranquero JA, Cazorla FM, de Vicente A. 2019. *Pseudomonas syringae* pv. syringae associated with mango trees, a particular pathogen within the "hodgepodge" of the *Pseudomonas syringae* complex. Front Plant Sci 10:570. https://doi.org/10.3389/fpls.2019.00570.
7. Young JM. 2010. Taxonomy of *Pseudomonas syringae*. J Plant Pathol 92:S5–S14. https://doi.org/10.4454/jpp.v92i1sup.2501.
8. Cazorla FM, Torés JA, Olalla L, Pérez-García A, Farré JM, De Vicente A. 1998. Bacterial apical necrosis of mango in southern Spain: a disease caused by *Pseudomonas syringae* pv. syringae. Phytopathology 88:614–620. https://doi.org/10.1094/PHYTO.1998.88.7.614.
9. Berge O, Monteil CL, Bartoli C, Chandeysson C, Guilbaud C, Sands DC, Morris CE. 2014. A user's guide to a database of the diversity of *Pseudomonas syringae* and its application to classifying strains in this phylogenetic complex. PLoS One 9:e105547. https://doi.org/10.1371/journal.pone.0105547.
10. Gutiérrez-Barranquero JA, Carrión VJ, Murillo J, Arrebola E, Arnold DL, Cazorla FM, De Vicente A. 2013. A *Pseudomonas syringae* diversity survey reveals a differentiated phylotype of the pathovar syringae associated with the mango host and mangotoxin production. Phytopathology 103:1115–1129. https://doi.org/10.1094/PHYTO-04-13-0093-R.
11. Lamichhane JR, Osdaghi E, Behlau F, Köhl J, Jones JB, Aubertot JN. 2018. Thirteen decades of antimicrobial copper compounds applied in agriculture. A review. Agron Sustain Dev 38:28. https://doi.org/10.1007/s13593-018-0503-9.
12. Iannotta N, Belfiore T, Brandmayr P, Noce ME, Scalercio S. 2007. Evaluation of the impact on entomocoenosis of active agents allowed in organic olive farming against *Bactrocera oleae* (Gmelin, 1790). J Environ Sci Health B 42:783–788. https://doi.org/10.1080/03601230701551020.
13. Kabata-Pendias A. 2010. Trace elements in soils and plants, 4th ed. CRC Press, New York, NY. https://doi.org/10.1201/b10158.
14. Xiong ZT, Wang H. 2005. Copper toxicity and bioaccumulation in Chinese cabbage (*Brassica pekinensis* Rupr.). Environ Toxicol 20:188–194. https://doi.org/10.1002/tox.20094.
15. Cazorla FM, Arrebola E, Sesma A, Pérez-García A, Codina JC, Murillo J, de Vicente A. 2002. Copper resistance in *Pseudomonas syringae* strains isolated from mango is encoded mainly by plasmids. Phytopathology 92:909–916. https://doi.org/10.1094/PHYTO.2002.92.8.909.
16. Vanneste JL, McLaren GE, Yu J, Conzish DA, Boyd R. 2005. Copper and streptomycin resistance in bacterial strains isolated from stone fruit orchards in New Zealand. NZPP 58:101–105. https://doi.org/10.30843/nzpp.2005.58.4262.
17. Behlau F, Canteros BI, Minsavage GV, Jones JB, Graham JH. 2011. Molecular characterization of copper resistance genes from *Xanthomonas citri*

subsp. *citri* and *Xanthomonas alfalfae* subsp. *citrumelonis*. Appl Environ Microbiol 77:4089–4096. https://doi.org/10.1128/AEM.03043-10.
18. Staehlin BM, Gibbons JG, Rokas A, O'Halloran TV, Slot JC. 2016. Evolution of a heavy metal homeostasis/resistance island reflects increasing copper stress in enterobacteria. Genome Biol Evol 8:811–826. https://doi.org/10.1093/gbe/evw031.
19. Colombi E, Straub C, Künzel S, Templeton MD, McCann HC, Rainey PB. 2017. Evolution of copper resistance in the kiwifruit pathogen *Pseudomonas syringae* pv. actinidiae through acquisition of integrative conjugative elements and plasmids. Environ Microbiol 19:819–832. https://doi.org/10.1111/1462-2920.13662.
20. Richard D, Ravigné V, Rieux A, Facon B, Boyer C, Boyer K, Grygiel P, Javegny S, Terville M, Canteros BI, Robène I, Vernière C, Chabirand A, Pruvost O, Lefeuvre P. 2017. Adaptation of genetically monomorphic bacteria: evolution of copper resistance through multiple horizontal gene transfers of complex and versatile mobile genetic elements. Mol Ecol 26:2131–2149. https://doi.org/10.1111/mec.14007.
21. Norman A, Hansen LH, Sørensen SJ. 2009. Conjugative plasmids: vessels of the communal gene pool. Philos Trans R Soc Lond B Biol Sci 364:2275–2289. https://doi.org/10.1098/rstb.2009.0037.
22. Johnson CM, Grossman AD. 2015. Integrative and conjugative elements (ICEs): what they do and how they work. Annu Rev Genet 49:577–601. https://doi.org/10.1146/annurev-genet-112414-055018.
23. Babakhani S, Oloomi M. 2018. Transposons: the agents of antibiotic resistance in bacteria. J Basic Microbiol 58:905–917. https://doi.org/10.1002/jobm.201800204.
24. Sundin GW. 2007. Genomic insights into the contribution of phytopathogenic bacterial plasmids to the evolutionary history of their hosts. Annu Rev Phytopathol 45:129–151. https://doi.org/10.1146/annurev.phyto.45.062806.094317.
25. Bardaji L, Pérez-Martínez I, Rodríguez-Moreno L, Rodríguez-Palenzuela P, Sundin GW, Ramos C, Murillo J. 2011. Sequence and role in virulence of the three plasmids complement of the model tumor-inducing bacterium *Pseudomonas savastanoi* pv. savastanoi NCPPB 3335. PLoS One 6:e25705. https://doi.org/10.1371/journal.pone.0025705.
26. Gutiérrez-Barranquero JA, Cazorla FM, de Vicente A, Sundin GW. 2017. Complete sequence and comparative genomic analysis of eight native *Pseudomonas syringae* plasmids belonging to the pPT23A family. BMC Genomics 18:1–17. https://doi.org/10.1186/s12864-017-3763-x.
27. Sesma A, Sundin GW, Murillo J. 2000. Phylogeny of the replication regions of pPT23A-like plasmids from *Pseudomonas syringae*. Microbiology 146:2375–2384. https://doi.org/10.1099/00221287-146-10-2375.
28. Mellano MA, Cooksey DA. 1988. Nucleotide sequence and organization of copper resistance genes from *Pseudomonas syringae* pv. tomato. J Bacteriol 170:2879–2883. https://doi.org/10.1128/jb.170.6.2879-2883.1988.
29. Cazorla FM, Codina JC, Abad C, Arrebola E, Torés JA, Murillo J, Pérez-García A, de Vicente A. 2008. 62-kb plasmids harboring *rulAB* homologues confer UV-tolerance and epiphytic fitness to *Pseudomonas syringae* pv. syringae mango isolates. Microb Ecol 56:283–291. https://doi.org/10.1007/s00248-007-9346-7.
30. Gutiérrez-Barranquero JA, de Vicente A, Carrión VJ, Sundin GW, Cazorla FM. 2013. Recruitment and rearrangement of three different genetic determinants into a conjugative plasmid increase copper resistance in *Pseudomonas syringae*. Appl Environ Microbiol 79:1028–1033. https://doi.org/10.1128/AEM.02644-12.
31. Kennelly MM, Cazorla FM, de Vicente A, Ramos C, Sundin GW. 2007. *Pseudomonas syringae* diseases of fruit trees: progress toward understanding and control. Plant Dis 91:4–17. https://doi.org/10.1094/PD-91-0004.
32. Cazorla FM, Arrebola E, Olea F, Velasco L, Hermoso JM, Pérez-García A, Torés JA, Farré JM, de Vicente A. 2006. Field evaluation of treatments for the control of the bacterial apical necrosis of mango (*Mangifera indica*) caused by *Pseudomonas syringae* pv. syringae. Eur J Plant Pathol 116:279–288. https://doi.org/10.1007/s10658-006-9059-7.
33. Gutiérrez-Barranquero JA, Arrebola E, Bonilla N, Sarmiento D, Cazorla FM, de Vicente A. 2012. Environmentally friendly treatment alternatives to Bordeaux mixture for controlling bacterial apical necrosis (BAN) of mango. Plant Pathol 61:665–676. https://doi.org/10.1111/j.1365-3059.2011.02559.x.
34. Behlau F, Hong JC, Jones JB, Graham JH. 2013. Evidence for acquisition of copper resistance genes from different sources in citrus-associated xanthomonads. Phytopathology 103:409–418. https://doi.org/10.1094/PHYTO-06-12-0134-R.
35. Ma Z, Smith JJ, Zhao Y, Jackson RW, Arnold DL, Murillo J, Sundin GW. 2007. Phylogenetic analysis of the pPT23A plasmid family of *Pseudomonas syringae*. Appl Environ Microbiol 73:1287–1295. https://doi.org/10.1128/AEM.01923-06.
36. Pérez-Martínez I, Zhao Y, Murillo J, Sundin GW, Ramos C. 2008. Global genomic analysis of *Pseudomonas savastanoi* pv. savastanoi plasmids. J Bacteriol 190:625–635. https://doi.org/10.1128/JB.01067-07.
37. Sundin GW, Bender CL. 1996. Molecular analysis of closely related copper- and streptomycin-resistance plasmids in *Pseudomonas syringae* pv. syringae. Plasmid 35:98–107. https://doi.org/10.1006/plas.1996.0012.
38. Jackson RW, Athanassopoulos E, Tsiamis G, Mansfield JW, Sesma A, Arnold DL, Gibbon MJ, Murillo J, Taylor JD, Vivian A. 1999. Identification of a pathogenicity island, which contains genes for virulence and avirulence, on a large native plasmid in the bean pathogen *Pseudomonas syringae* pathovar phaseolicola. Proc Natl Acad Sci U S A 96:10875–10880. https://doi.org/10.1073/pnas.96.19.10875.
39. Sundin GW, Murillo J. 1999. Functional analysis of the *Pseudomonas syringae rulAB* determinant in tolerance to ultraviolet B (290–320 nm) radiation and distribution of *rulAB* among *P syringae* pathovars. Environ Microbiol 1:75–87. https://doi.org/10.1046/j.1462-2920.1999.00008.x.
40. Vivian A, Murillo J, Jackson RW. 2001. The roles of plasmids in phytopathogenic bacteria: mobile arsenals? Microbiology (Reading) 147:763–780. https://doi.org/10.1099/00221287-147-4-763.
41. Sundin GW, Kidambi SP, Ullrich M, Bender CL. 1996. Resistance to ultraviolet light in *Pseudomonas syringae*: sequence and functional analysis of the plasmid-encoded *rulAB* genes. Gene 177:77–81. https://doi.org/10.1016/0378-1119(96)00273-9.
42. Sundin GW, Jacobs JL, Murillo J. 2000. Sequence diversity of *rulA* among natural isolates of *Pseudomonas syringae* and effect on function of *rulAB*-mediated UV radiation tolerance. Appl Environ Microbiol 66:5167–5173. https://doi.org/10.1128/aem.66.12.5167-5173.2000.
43. Arredondo-Alonso S, Top J, McNally A, Puranen S, Pesonen M, Pensar J, Marttinen P, Braat JC, Rogers MRC, van Schaik W, Kaski S, Willems RJL, Corander J, Schürch AC. 2020. Plasmids shaped the recent emergence of the major nosocomial pathogen *Enterococcus faecium*. mBio 11:e03284-19. https://doi.org/10.1128/mBio.03284-19.
44. Parks AR, Peters JE. 2009. Tn7 elements: engendering diversity from chromosomes to episomes. Plasmid 61:1–14. https://doi.org/10.1016/j.plasmid.2008.09.008.
45. Peters JE, Craig NL. 2001. Tn7: smarter than we thought. Nat Rev Mol Cell Biol 2:806–814. https://doi.org/10.1038/35099006.
46. Peters JE. 2019. Targeted transposition with Tn7 elements: safe sites, mobile plasmids, CRISPR/Cas and beyond. Mol Microbiol 112:1635–1644. https://doi.org/10.1111/mmi.14383.
47. Cazorla FM, Olalla L, Torés JA, Pérez-Garcí A, Codina JC, de Vicente A. 1995. A method for estimation of population densities of ice nucleating active *Pseudomonas syringae* in buds and leaves of mango. J Appl Bacteriol 79:341–346. https://doi.org/10.1111/j.1365-2672.1995.tb03146.x.
48. Sorensen KN, Kim KH, Takemoto JY. 1998. PCR detection of cyclic lipodepsinonapeptide-producing *Pseudomonas syringae* pv. syringae and similarity of strains. Appl Environ Microbiol 64:226–230. https://doi.org/10.1128/AEM.64.1.226-230.1998.
49. Gross DC, DeVay JE. 1977. Population dynamics and pathogenesis of *Pseudomonas syringae* in maize and cowpea in relation to the in vitro production of syringomycin. Phytopathology 77:475–483. https://doi.org/10.1094/Phyto-67-475.
50. Arrebola E, Cazorla FM, Durán VE, Rivera E, Olea F, Codina JC, Pérez-García A, de Vicente A. 2003. Mangotoxin: a novel antimetabolite toxin produced by *Pseudomonas syringae* inhibiting ornithine/arginine biosynthesis. Physiol Mol Plant Pathol 63:117–127. https://doi.org/10.1016/j.pmpp.2003.11.003.
51. Carrión VJ, Gutiérrez-Barranquero JA, Arrebol E, Bardaji L, Codina JC, de Vicente A, Cazorla FM, Murillo J. 2013. The mangotoxin biosynthetic operon (*mbo*) is specifically distributed within *Pseudomonas syringae* genomospecies 1 and was acquired only once during evolution. Appl Environ Microbiol 79:756–767. https://doi.org/10.1128/AEM.03007-12.
52. Moulton PJ, Vivian A, Hunter PJ, Taylor JD. 1993. Changes in cultivar-specificity toward pea can result from transfer of plasmid RP4 and other incompatibility group P1 replicons to *Pseudomonas syringae* pv. pisi. J Gen Microbiol 139:3149–3155. https://doi.org/10.1099/00221287-139-12-3149.
53. Murillo J, Shen H, Gerhold D, Sharma A, Cooksey DA, Keen NT. 1994. Characterization of pPT23B, the plasmid involved in syringolide production by *Pseudomonas syringae* pv. tomato PT23. Plasmid 31:275–287. https://doi.org/10.1006/plas.1994.1029.
54. Murillo J, Bardaji L, Navarro de la Fuente L, Führer ME, Aguilera S, Álvarez-

Morales A. 2011. Variation in conservation of the cluster for biosynthesis of the phytotoxin phaseolotoxin in *Pseudomonas syringae* suggests at least two events of horizontal acquisition. Res Microbiol 162:253–261. https://doi.org/10.1016/j.resmic.2010.10.011.
55. Kumar S, Stecher G, Tamura K. 2016. MEGA7: molecular evolutionary genetics analysis version 7.0 for bigger datasets. Mol Biol Evol 33:1870–1874. https://doi.org/10.1093/molbev/msw054.
56. Falgueras J, Lara AJ, Fernández-Pozo N, Cantón FR, Pérez-Trabado G, Claros MG. 2010. SeqTrim: a high-throughput pipeline for pre-processing any type of sequence read. BMC Bioinformatics 11:38. https://doi.org/10.1186/1471-2105-11-38.
57. Coil D, Jospin G, Darling AE. 2015. A5-miseq: an updated pipeline to assemble microbial genomes from Illumina MiSeq data. Bioinformatics 31:587–589. https://doi.org/10.1093/bioinformatics/btu661.
58. Martínez-García PM, Rodríguez-Palenzuela P, Arrebola E, Carrión VJ, Gutiérrez-Barranquero JA, Pérez-García A, Ramos C, Cazorla FM, de Vicente A. 2015. Bioinformatics analysis of the complete genome sequence of the mango tree pathogen *Pseudomonas syringae* pv. syringae UMAF0158 reveals traits relevant to virulence and epiphytic lifestyle. PLoS One 10:e0136101. https://doi.org/10.1371/journal.pone.0136101.
59. Heredia-Ponce Z, Gutiérrez-Barranquero JA, Purtschert-Montenegro G, Eberl L, Cazorla FM, de Vicente A. 2020. Biological role of EPS from *Pseudomonas syringae* pv. syringae UMAF0158 extracellular matrix, focusing on a Psl-like polysaccharide. NPJ Biofilms Microbiomes 6:37. https://doi.org/10.1038/s41522-020-00148-6.
60. Young A. 2008. Notes on *Pseudomonas syringae* pv. syringae bacterial necrosis of mango (*Mangifera indica*) in Australia. Austral Plant Dis Notes 3:138–140. https://doi.org/10.1071/DN08053.
61. Gutiérrez-Barranquero JA, Arrebola E, Pérez-García A, Codina JC, Murillo J, de Vicente A, Cazorla FM. 2008. Evaluation of phenotypic and genetic techniques to analyze diversity of *Pseudomonas syringae* pv. syringae strains isolates from mango trees, p 271–281. *In* Fatmi MB, Collmer A, Iacobellis NS, Mansfield JW, Murillo J, Schaad NW, Ullrich M (ed), *Pseudomonas syringae* pathovars and related pathogens—identification, epidemiology and genomics. Springer Netherlands, Dordrecht, The Netherlands.
62. Aiello D, Ferrante P, Vitale A, Polizzi G, Scortichini M, Cirvilleri G. 2015. Characterization of *Pseudomonas syringae* pv. syringae isolated from mango in Sicily and occurrence of copper-resistant strains. J Plant Pathol 97:273–282. https://doi.org/10.4454/JPP.V97I2.015.
63. Baltrus DA, Nishimura MT, Romanchuk A, Chang JH, Mukhtar MS, Cherkis K, Roach J, Grant SR, Jones CD, Dangl JL. 2011. Dynamic evolution of pathogenicity revealed by sequencing and comparative genomics of 19 *Pseudomonas syringae* isolates. PLoS Pathog 7:e1002132. https://doi.org/10.1371/journal.ppat.1002132.
64. Teverson DM. 1991. PhD thesis. Genetics of pathogenicity and resistance in the halo-blight disease of beans in Africa. University of Birmingham, Birmingham, UK.
65. Hirano SS, Charkowski A, Collmer A, Willis DK, Upper CD. 1999. Role of the Hrp type III protein secretion system in growth of *Pseudomonas syringae* B728a on host plant in the field. Proc Natl Acad Sci U S A 96:9851–9856. https://doi.org/10.1073/pnas.96.17.9851.
66. Cuppels DA. 1986. Generation and characterization of Tn5 insertion mutations in *Pseudomonas syringae* pv. tomato. Appl Environ Microbiol 51:323–327. https://doi.org/10.1128/AEM.51.2.323-327.1986.